REVISTA URBANO Nº 49 / MAYO 2024 - OCTUBRE 2024
PÁG. 8 - 23
ISSN 0717 - 3997 / 0718 - 3607

Recibido: 25-09-2023
Aceptado: 01-05-2024

SPATIAL-TEMPORAL ANALYSIS OF HEAT ISLANDS APPLIED TO THE COASTAL CITY OF SAN FRANCISCO DE CAMPECHE, MEXICO [1]

ANÁLISIS ESPACIOTEMPORAL DE ISLAS DE CALOR APLICADO EN LA CIUDAD COSTERA DE SAN FRANCISCO DE CAMPECHE, MÉXICO

ROMÁN CANUL-TURRIZA [2]
KARIANNA AKÉ-TURRIZA [3]
OSCAR MAY-TZUC [4]
MARIO JIMÉNEZ-TORRES [5]

1 This work is part of the “San Francisco de Campeche Climatological Observatory “ research project (Stage 01)” project 036/ UAC/2023 of the Autonomous University of Campeche.

2 Doctor en Ingeniería
Profesor – Investigador de la Facultad de Ingeniería.
Universidad Autónoma de Campeche, San Francisco de Campeche, México.
https://orcid.org/0000-0003-2081-9913
roacanul@uacam.mx

3 Magíster en Proyectos de Arquitectura y Urbanismo
Estudiante de la Facultad de Ciencias Químico Biológicas
Instituto de Ecología, Pesquerías y Oceanografía del Golfo de México, San Francisco de Campeche, México.
https://orcid.org/0009-0001-6598-216X
al041220@uacam.mx

4 Doctor en Ingeniería
Profesor-Investigador de la Facultad de Ingeniería
Universidad Autónoma de Campeche, San Francisco de Campeche, México.
https://orcid.org/0000-0001-7681-8210
oscajmay@uacam.mx

5 Doctor en Ingeniería
Profesor de la Facultad de Ingeniería
Universidad Autónoma de Campeche, San Francisco de Campeche, México.
https://orcid.org/0000-0002-8331-1888
majimene@uacam.mx

https://doi.org/10.22320/07183607.2024.27.49.01

ANÁLISIS ESPACIOTEMPORAL DE ISLAS DE CALOR APLICADO EN LA CIUDAD COSTERA DE SAN FRANCISCO DE CAMPECHE, MÉXICO
ROMÁN CANUL-TURRIZA, KARIANNA AKÉ-TURRIZA, OSCAR MAY-ITZUC, MARIO JIMÉNEZ-TORRES
REVISTA URBANO Nº 49 / MAYO 2024 - OCTUBRE 2024
PÁG. 8 - 23
ISSN 0717 - 3997 / 0718 - 3607

La urbanización de la ciudad de San Francisco de Campeche influye en la formación de isla de calor urbano debido a materiales de construcción, edificios y estructuras, actividades humanas, falta de vegetación, e infraestructura de transporte. Las islas de calor tienen consecuencias negativas como aumento en el consumo de energía y un mayor estrés térmico en la población. Además, contribuyen al cambio climático debido al aumento de emisiones de gases de efecto invernadero, causadas por la demanda adicional de energía. Ciudades como Sídney, Beijing, Nanjing, Moscú y Hong Kong están implementando estrategias de planificación urbana que promueven la vegetación urbana, el uso de materiales de construcción reflectantes, la mejora del transporte público y la promoción de la eficiencia energética en edificios. Con el fin de identificar islas de calor se utilizaron imágenes satelitales Landsat. Se analizó el crecimiento de la población y la mancha urbana realizando un análisis de índice de vegetación. En relación con los análisis realizados, se identificó que la temperatura ha aumentado aproximadamente 6°C entre los años 1990 y 2022; así como ha disminuido la vegetación ante el crecimiento de la mancha urbana y las viviendas, cuadruplicando el Índice de Vegetación de Diferencia Normalizada (NDVI) en la clase 0-0.25. Finalmente, se proponen medidas de mitigación para contrarrestar los efectos que causan las islas de calor en la ciudad.

Palabras clave: islas, calor, ciudad, costa

The urbanization of the city of San Francisco de Campeche influences the formation of urban heat islands due to construction materials, buildings and structures, human activities, lack of vegetation, and transportation infrastructure. Heat islands have negative consequences such as increased energy consumption and heat stress for the population, contributing to climate change due to increased greenhouse gas emissions caused by additional energy demand. Cities such as Sydney, Beijing, Nanjing, Moscow, and Hong Kong are implementing urban planning strategies that promote urban vegetation, the use of reflective building materials, the improvement of public transport, and the promotion of energy efficiency in buildings. Landsat satellite images were used to analyze population growth and urban sprawl to identify heat islands, and a vegetation index analysis was also made. Regarding the analyses, it was recognized that the temperature increased by approximately 6°C between 1990 and 2022. There has also been a decrease in vegetation due to the urban sprawl and housing growth, quadrupling the Normalized Difference Vegetation Index (NDVI) in the 0-0.25 class for the same period. Finally, mitigation measures are proposed to counteract the effects caused by heat islands in the city.

Keywords: islands, heat, city, coastline

ANÁLISIS ESPACIOTEMPORAL DE ISLAS DE CALOR APLICADO EN LA CIUDAD COSTERA DE SAN FRANCISCO DE CAMPECHE, MÉXICO
ROMÁN CANUL-TURRIZA, KARIANNA AKÉ-TURRIZA, OSCAR MAY-TZUC, MARIO JIMÉNEZ-TORRES
REVISTA URBANO Nº 49 / MAYO 2024 - OCTUBRE 2024
PÁG. 8 - 23
ISSN 0717 - 3997 / 0718 - 3607

I. INTRODUCTION

Urbanization is one of the human processes with the most significant environmental and climate impact. 55% of the world's population lives in cities, which is expected to increase to 68% by 2050 (Ma et al., 2023). Harmful agents for health are emitted, which affect local meteorology. At the same time, urban growth, economic development, and changes in land use are also a threat to humans and the ecosystem (Xu et al., 2021), as cities contribute to global warming, mainly due to the effect of Urban Heat Islands or UHI.

For example, in the coastal regions of the world, the effect of the UHI is extreme, changing the regional meteorology with extreme heat waves and floods, and the phenomenon is expected to intensify (Qiu et al., 2023). In these regions, the complexity increases as a result of the sea breeze that leads the UHI several kilometers inland until its dissipation (Yun et al., 2020). It is necessary to understand the phenomenology to allow the formulation of policies supporting decision-making and scenario planning that consider: a) Analysis of the time scale; b) Inclusion of landscape and urban form, proportion of green and blue areas, improvement of the albedo, modal distribution of transport; c) Passive technologies in the building envelope; d) Active technologies considering artificial climate control; and e) Public health and citizen participation (Degirmenci et al., 2021). Therefore, focusing on urban decentralization, expansion control, green coverage rate, and building density will improve the thermal environment and air pollution (Luo & He, 2021).

Currently, there is a lack of knowledge about the spatio-temporal variation of the intensity of daytime and nighttime surface UHI. Similarly, resources still need to be improved to cope with the rapid impacts of urbanization. In recent years, satellite images have been used as an alternative to detect UHIs due to their availability, free access, and extensive registration history. San Francisco de Campeche is an essential region because it belongs to the World Heritage list and is located in a coastal area with rapid urbanization, so conducting a study focused on the UHI, using satellite images from the period 1990 – 2020, will quantify the historical changes in surface and atmospheric temperature, as well as changes in vegetation cover, to identify and characterize the UHI. It is also hypothesized that the results of this study will reveal the areas with the most significant changes in temperature and vegetation cover, thus providing a basis for proposing actions to mitigate the effects of UHI in San Francisco de Campeche.

II. THEORETICAL FRAMEWORK

Urban Heat Islands (UHI)

UHI are thermal anomalies resulting from the temperature difference between a surrounding urban and rural area, where the additional heat emitted increases the atmospheric temperature (Ortiz Porangaba et al., 2021). These increase summer cooling loads and consequent energy consumption, which leads to higher greenhouse gas emissions (Khare et al., 2021). This thermal process affects the population by increasing the local temperature and by releasing pollutants into the atmosphere and air pollution. Therefore, it is vital to understand how the components of cities relate to UHIs to establish improvement measures in the urban thermal environment and to reduce air pollution (Kim & Brown, 2021; Liang et al., 2021). With the rapid spread of urbanization worldwide, the urban heat island effect substantially and adversely impacts cities, including energy, environment, and health conditions. Unfortunately, constructive geometry and human activities severely intensify the phenomenon of UHIs (Xu et al., 2021).

It has also been observed that UHIs and air pollution are responsible for significant health impacts. According to a World Health Organization (WHO) report, indoor air pollution caused approximately 3.8 million deaths in 2016, and about 4.2 million deaths were attributed to air pollution in the same year. In addition, it is estimated that 91% of the population lives where the air quality index exceeds the limits of the WHO guidelines. Therefore, regarding the figures provided by the WHO, regulating urbanization could have two-way benefits (Singh et al., 2020). Urbanization coincides with notable environmental changes, including vegetation, soil, and climate (Vasenev et al., 2021). Therefore, understanding how the components of cities affect UHIs has become a great challenge for societies that seek to improve the quality of life through the implementation of urban planning criteria (Hidalgo García & Arco Díaz, 2021).

The selection of urban planning indicators such as building density, built area, and green coverage rate, among others, during the preparation phase for urban planning, can regulate the intensity of urban development and the configuration of the urban thermal environment after the application of the planning proposal (Luo & He, 2021). This understanding of the relationship between urban planning indicators and the formation of the term environment allows addressing, in greater detail, the thermal aspect in the planning stage, which helps optimize the urban

ANÁLISIS ESPACIOTEMPORAL DE ISLAS DE CALOR APLICADO EN LA CIUDAD COSTERA DE SAN FRANCISCO DE CAMPECHE, MÉXICO
ROMÁN CANUL-TURRIZA, KARIANNA AKÉ-TURRIZA, OSCAR MAY-TZUC, MARIO JIMÉNEZ-TORRES
REVISTA URBANO Nº 49 / MAYO 2024 - OCTUBRE 2024
PÁG. 8 - 23
ISSN 0717 - 3997 / 0718 - 3607

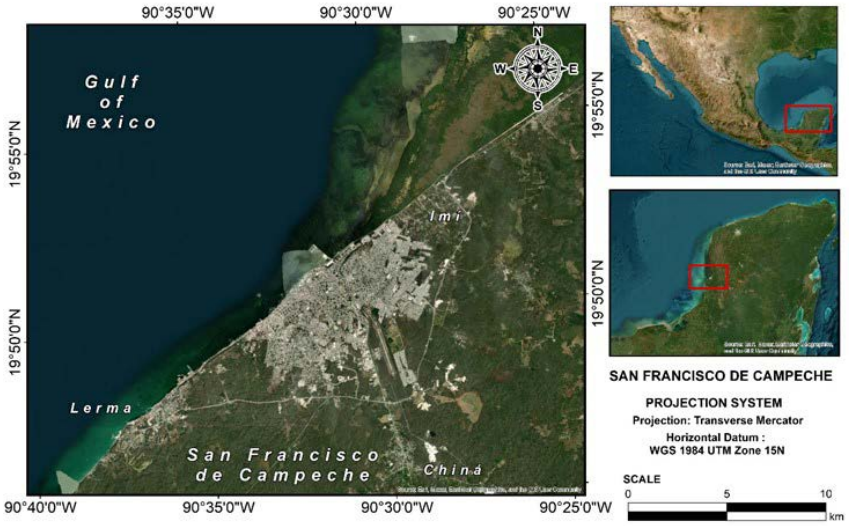

Figure 1. Location of the city of SFC, Mexico. Source: Preparation by the authors.

planning proposal to mitigate the effects of UHIs (Luo & He, 2021).

Even though urban areas face multiple environmental challenges interacting with climate change, including the UHI effect, vegetation can be a nature-based solution for UHI mitigation (Tan et al., 2021). The interaction of UHI in a coastal tropical city may be different from that of cities in temperate climate zone, affecting it severely. However, there is a lack of UHI studies focused on coastal tropical cities (Chew et al., 2021).

Internationally, some studies have been carried out worldwide in coastal cities such as those of Greece (Giannaros & Melas, 2012), Oman (Charabi and Bakhit, 2011), in the Caspian Sea (Firozjaei et al., 2023), Istanbul (Dihkan et al., 2015), China (X. Xu et al., 2023) and in the Mediterranean Sea (Kassomenos et al., 2022). However, studies are still emerging in Mexico and the Gulf of Mexico.

III. CASE STUDY

Case study: Campeche, Mexico

The study was conducted in San Francisco de Campeche (SFC) (19°50'41'N and 90°32'23'W), the State Capital of Campeche, Mexico, which is located on the Yucatan Peninsula, on the shores of the Gulf of Mexico (Figure 1).

San Francisco de Campeche is a fortified historical city and one of the few walled cities in America. Its historic center and old neighborhoods have buildings dating from the sixteenth to the nineteenth centuries, including military, civil, and religious architecture. Given its historical and commercial context, the homogeneity of its architecture was declared an Area of Historical Monuments in 1986, and in 1999, it was included in the list of World Heritage of Humanity of the United Nations Educational, Scientific, and Cultural Organization (UNESCO).

It has an area of 3,410.64 km^2 with an average altitude of 5 meters above sea level (Figure 1). It is mainly characterized by a warm-humid climate with summer rains, which are distributed in three seasons: "Rains" (June-September), "Norths" (October-January), and "Dry" (February-May). The city's average annual temperature is 27°C, with maximum summer averages of 29°C and a historical maximum temperature of 43°C (INEGI, 2022).

Demographically, it has 294,077 inhabitants, 32% of the State's inhabitants, with a population increase of 25% in the last ten years (INEGI, 2020). This has led to unplanned urbanization, which originated from transforming land into housing areas, thus reducing the green areas within the city. These areas are identified as having UHI potential, generating an urban increase in the use of air conditioning, energy demand, and air pollution.

This type of urban growth pattern in San Francisco de Campeche is primarily associated with high energy consumption, which is why this city is considered a case study whose analysis will help generate a methodology that allows

ANÁLISIS ESPACIOTEMPORAL DE ISLAS DE CALOR APLICADO EN LA CIUDAD COSTERA DE SAN FRANCISCO DE CAMPECHE, MÉXICO
ROMÁN CANUL-TURRIZA, KARIANNA AKÉ-TURRIZA, OSCAR MAY-TZUC, MARIO JIMÉNEZ-TORRES
REVISTA URBANO Nº 49 / MAYO 2024 - OCTUBRE 2024
PÁG. 8 - 23
ISSN 0717 - 3997 / 0718 - 3607

detecting and proposing exportable improvements to other cities with similar characteristics, such as addressing public health problems, improving energy efficiency, protecting the environment, and adapting to climate change.

IV. METHODOLOGY

To identify and characterize UHIs from a temporal perspective and to contrast them with population growth, it is proposed to break down the analysis into four phases: (1) Analyze the population growth of the city of SFC; (2) Quantify the historical temperature changes (surface and atmospheric); (3) Quantify the changes in vegetation cover; and (4) Identify the areas with the most significant changes in temperature, vegetation cover and the relationship between them. Therefore, the methodology analyzes four temporal elements: the Land Surface Temperature or LST, Normalized Difference Vegetation Index or NDVI, historical population growth, and analysis of the local temperature history, the latter to reinforce the analysis of temperature changes.

The historical climate analysis used data from the ERA5 model generated by the European Center for Medium-term Weather Prediction and local weather stations. The population analysis is based on the region's demographic records.

Landsat satellite images, represented in spectral bands, were used to calculate the LST and NDVI. Due to the scarce information available and the precarious monitoring and observation systems of local environmental changes, these images are essential for analyzing and addressing environmental problems in Latin American cities. Landsat-5TM, Landsat-7TM, Landsat-8OLI, and Landsat-9OLI images were examined. They were obtained from the databases of the United States Geological Survey (USGS, no date). The study analyzed images between 1990 and 2020 in 5-year intervals associated with April to characterize the dry season, which is the hottest in the region.

Historical growth of the population of the urban conurbation area

Data were collected from population growth and its relationship with the urbanized area. These were collected from local records, such as the Municipal Urban Development Program of Campeche 2020-2040 (SEDATU, 2020), the Campeche Urban Development Director Program 2008-2033 (PDU, in Spanish), and the Municipal Program of Territorial Ecological Management (PMOET, in Spanish).

Earth's surface temperature

To obtain this data, images of band 6 were used for Landsat-5TM and Landsat-7TM, and band 10 for Landsat-8OLI and Landsat-9OLI. The calculation consists of 4 steps (X. Li et al., 2016) :

1. *Spectral radiance* $(L_\lambda, W/(m^2 sr * \mu m))$ for TM images is obtained with Eq.1, where is the digital value of the pixel in a range of 0-255, and , the maximum and minimum values of the pixels in the thermal band, and and , the scaled maximum and minimum spectral radiances. For the OLI images, this was calculated from Eq.2 (considering radiation at the top of the atmosphere or TOA radiance), where was the correction for band 10, and *ML* and *AL* represented multiplicative and additive factors for the reheating of the radiance to a certain band.

$$L_\lambda = \left(\frac{L_{max,\lambda} - L_{min,\lambda}}{Q_{cal,max} - Q_{cal,min}}\right) * (Q_{cal} - Q_{cal,min}) + L_{min,\lambda} \quad (1)$$

$$L_\lambda = ML * Q_{cal} + AL - O_i \quad (2)$$

2. *Luminous intensity temperature or Bright Temperature (BT)* Eq.3, where K1 and K2 are thermal conversion constants associated with the type of satellite image (TM or OLI).

$$BT = \frac{K2}{ln\left(\frac{K1}{L_\lambda} + 1\right)} - 273.15°C \quad (3)$$

3. *Land Surface Emissivity (LSE)* Eq.4, indicates the average emissivity of an element on the land surface from the NDVI, where and are the maximum and minimum of the *NDVI*.

$$LSE = 0.004 * \left(\frac{NDVI - NDVI_{min}}{NDVI_{max} - NDVI_{min}}\right)^2 + 0.986 \quad (4)$$

4. *Estimation of the LST*, given by Eq.5, where is the wavelength of the emitted radiance (µm), *h=; s* is Boltzman's constant, and *c* is the speed of light.

$$LST = \frac{BT}{\left(1 + \left(\lambda * \frac{BT}{h * c/s}\right) * \ln(LSE)\right)} \quad (5)$$

Surface temperature time series

For this analysis, the temperature record from 1940 to 2023 was used, obtained from two sources:

- From 1940-2022, from the ERA5 model (https://cds.climate.copernicus.eu), for air temperature records at 2 m above the Earth's surface to identify increases in the city over time. This value is calculated in one-hour intervals by interpolating between the lowest level of the model and the land surface.

ANÁLISIS ESPACIOTEMPORAL DE ISLAS DE CALOR APLICADO EN LA CIUDAD COSTERA DE SAN FRANCISCO DE CAMPECHE, MÉXICO
ROMÁN CANUL-TURRIZA, KARIANNA AKÉ-TURRIZA, OSCAR MAY-TZUC, MARIO JIMÉNEZ-TORRES
REVISTA URBANO Nº 49 / MAYO 2024 - OCTUBRE 2024
PÁG. 8 - 23
ISSN 0717 - 3997 / 0718 - 3607

- 2022-2023, from a multifunctional wireless weather station located within the city at the coordinates 19.85°N – 90.50°W. The temperature data series was collected from October 2022 to April 2023, recording every 10 minutes.

Normalized difference vegetation index

1. This indicator checks the condition of vegetation from near-infrared (NIR) and red (R) bands from the Landsat images. Its estimation was made through the following formula Eq. 6 (H. Li et al., 2018):

$$NDVI = (NIR - R)/(NIR + R) \quad (6)$$

For the Landsat-5TM and Landsat-7TM images, spectral bands 4 and 3 were used for the NIR and R values, while for Landsat-8OLI and Landsat-9OLI, bands 5 and 6 apply. The NDVI values range between ±1.0, while green vegetation is between the values of 0.2-0.8 (Wang et al., 2020).

V. RESULTS

Analysis of historical population growth

Figure 2 presents the historical demographic growth, built housing, and impact on urban fragmentation in the city from 1950 to 2019 (last census). Figure 2 contrasts the city's population growth concerning built-up housing. Over the 70 years, the state's population has grown by 87%, with the highest increases occurring in 1970 and 2019. A third of the increase has happened in the last ten years. On the other hand, the number of housing units has grown even faster, increasing by 91% since 1980. In particular, real estate expansion has grown by 38% since 2000, which is associated with demographic growth. These results are linked to the increase in urban sprawl (Figure 2), a product of urban expansion to the south and east of the city. In the eighties and nineties, housing growth was concentrated in the southern and southeastern areas. Changes in land use are directly associated with the increase in land temperature.

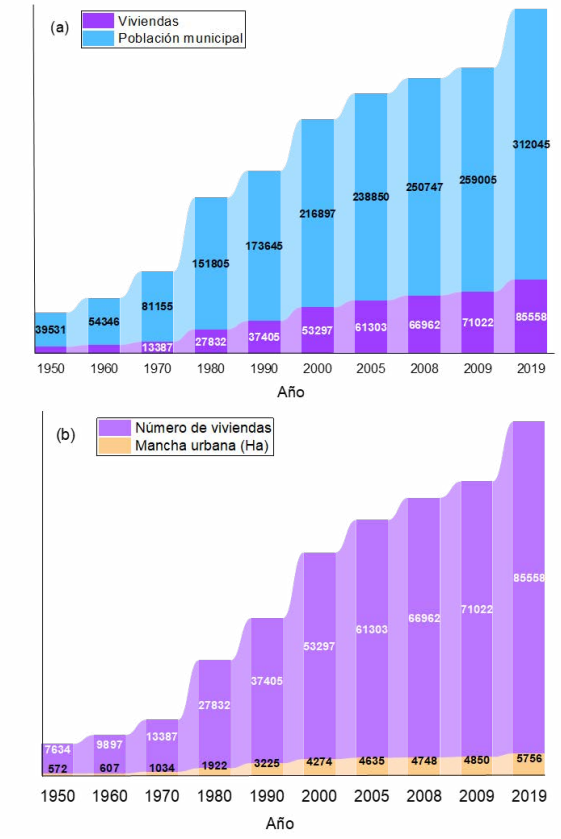

Figure 2. a) Housing behavior and urban sprawl in Campeche (above), b) Housing behavior compared to the population of Campeche (below). Source: Preparation by the authors.

Land surface temperature (LST)

Figure 3 compiles the LST maps from 1990 to 2020 in five-year intervals, cataloging the surface temperature in 5 color ranges: Blue (< 20°C), light blue (20-25°C), green (25-30°C), yellow (30-35°C), orange (35-40°C), and red (>40°C). During the nineties, the city did not exceed 25°C at a land level at the hottest time of the year, with the oldest and most central neighborhoods having higher temperatures, a product of the reduced urban sprawl. In later decades (2000-2020), the LST exceeded 30°C due to urban expansion to the city's surrounding areas. This is consistent with the emergence of housing neighborhoods in the east and west, which caused an expansion of 37% on forest land.

In the areas of the historical center and the east, an increase in temperature caused by deforestation was observed, exceeding 35°C. In addition, the tendency to generate zones that reach or exceed 40°C is interesting. This indicates that, in 30 years, a coastal city with a small population, such as the case study, has increased the land-level temperature by approximately 10°C.

To visualize the behavior of the temperature at ground level, information was extracted from 24 points identified with more significant change throughout the city for each of the

ANÁLISIS ESPACIOTEMPORAL DE ISLAS DE CALOR APLICADO EN LA CIUDAD COSTERA DE SAN FRANCISCO DE CAMPECHE, MÉXICO
ROMÁN CANUL-TURRIZA, KARIANNA AKÉ-TURRIZA, OSCAR MAY-TZUC, MARIO JIMÉNEZ-TORRES
REVISTA URBANO Nº 49 / MAYO 2024 - OCTUBRE 2024
PÁG. 8 - 23
ISSN 0717 - 3997 / 0718 - 3607

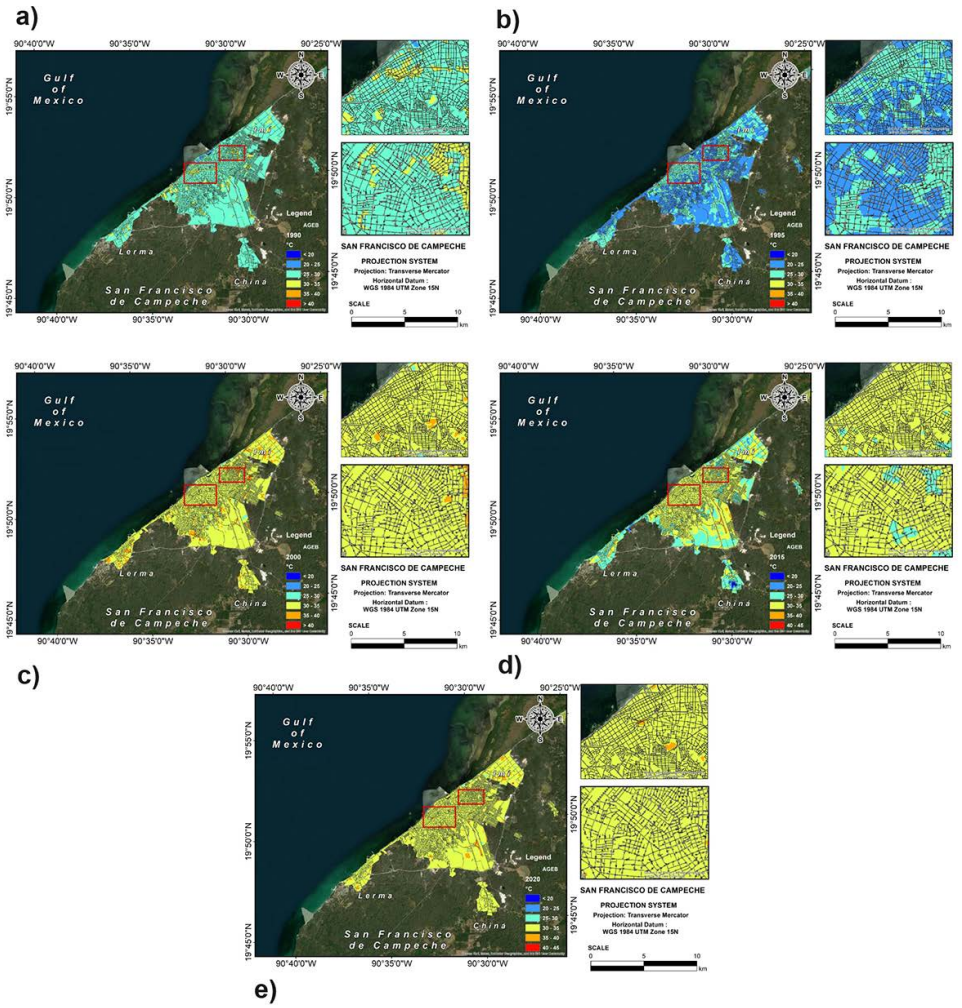

Figure 3. Land temperature maps for the case study: a)1990; b)1995; c)2000; d)2015; e)2020. Source: Preparation by the authors.

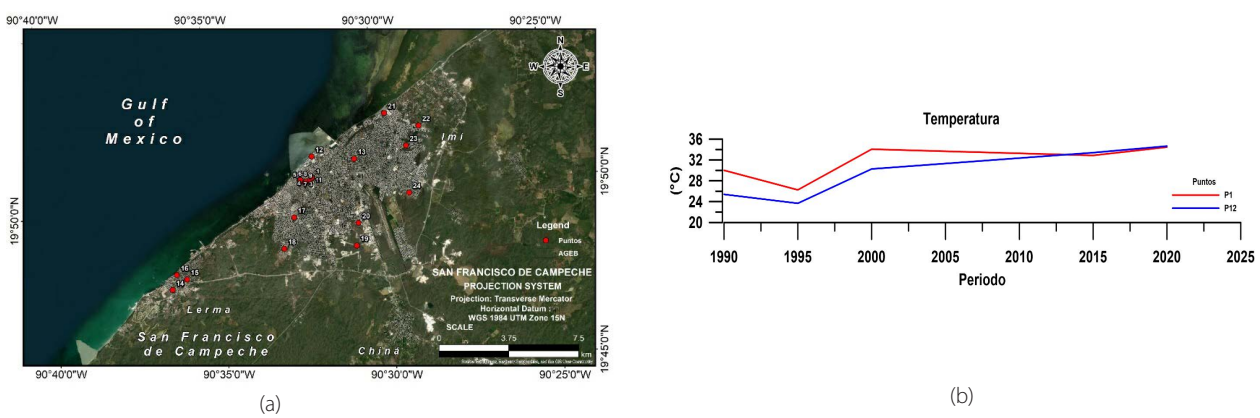

Figure 4. Information extraction points and Series for points 1 and 12. Source: Preparation by the authors.

ANÁLISIS ESPACIOTEMPORAL DE ISLAS DE CALOR APLICADO EN LA CIUDAD COSTERA DE SAN FRANCISCO DE CAMPECHE, MÉXICO
ROMÁN CANUL-TURRIZA, KARIANNA AKÉ-TURRIZA, OSCAR MAY-ITZUC, MARIO JIMÉNEZ-TORRES
REVISTA URBANO Nº 49 / MAYO 2024 - OCTUBRE 2024
PÁG. 8 - 23
ISSN 0717 - 3997 / 0718 - 3607

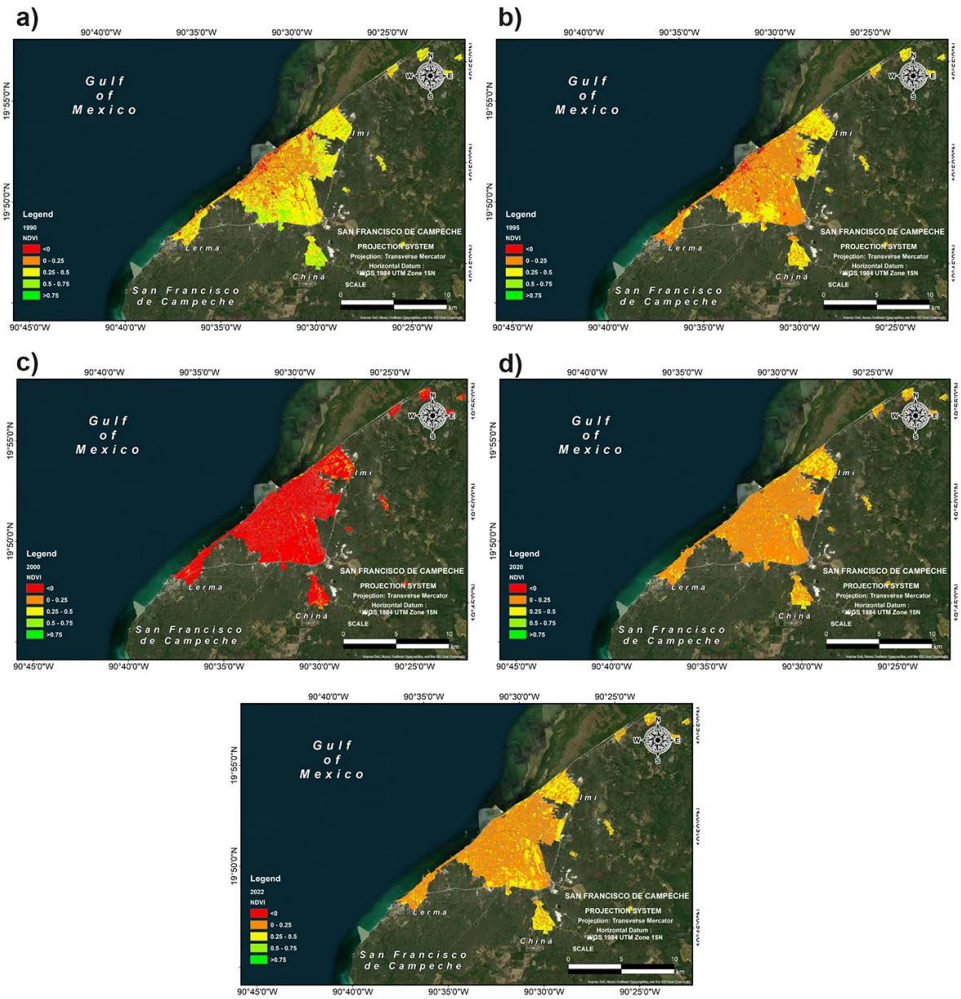

Figure 5. NDVI maps for the case study: a)1990; b) 1995; c)2000; d)2020; e)2022. Source: Preparation by the authors.

analyzed images (Figure 4). The graph shows the changes in temperature for points 1 and 12, with an average increase of 6°C from 1990 to 2020.

Vegetation analysis

The NDVI values were grouped into five vegetation classes: Very scarce (<0), scarce (0-0.25), reduced (0.25-0.50), acceptable (0.50-0.75), and abundant (>0.75), as can be seen in Figure 5. Figure 4 shows that, in 1990, the urban area was reduced and concentrated in the city center, with sparse vegetation dominating. However, a significant portion of what at that time represented the city's periphery (currently the southern and eastern areas) retained acceptable levels of vegetation. Five years later, a reduction in vegetation is visible in the east of the city, coinciding with the demographic increase and the number of buildings. In 2020, the reduction of vegetation extended to the south and southeast of the city, where more than 90% of the urban core is in the category of scarce vegetation, contributing to the rise in temperature.

Table 1 compiles the evolution of the NDVI in the last 20 years. The least frequent category that has been reduced the most is "very scarce vegetation," which has gone from 16.38ha to 0.38ha. On the other hand, the "scarce" category has been the most representative and the only one that has grown, while the extensions in the "abundant" vegetation category are almost imperceptible. During these two decades, there has been a tendency to reduce urban vegetation, putting the population at risk from the tropical climate heat waves without green areas or urban vegetation to cushion them.

ANÁLISIS ESPACIOTEMPORAL DE ISLAS DE CALOR APLICADO EN LA CIUDAD COSTERA DE SAN FRANCISCO DE CAMPECHE, MÉXICO
ROMÁN CANUL-TURRIZA, KARIANNA AKÉ-TURRIZA, OSCAR MAY-TZUC, MARIO JIMÉNEZ-TORRES
REVISTA URBANO Nº 49 / MAYO 2024 - OCTUBRE 2024
PÁG. 8 - 23
ISSN 0717 - 3997 / 0718 - 3607

Classes	Area in Hectares					
	1990	1995	2000	2015	2020	2022
<0	116.45	16.52	579.16	0.32	0.14	0.38
0-0.25	181.75	386.60	54.27	410.3	515.75	433.59
0.25-0.5	371.60	230.85	1.76	224.4	119.29	200.94
0.5-0.75	65.36	1.22	0	0.17	0.01	0.27
>0.75	0	0	0	0	0	0

Table 1. Details of the normalized difference vegetation index from 1990 to 2022. Source: Preparation by the authors.

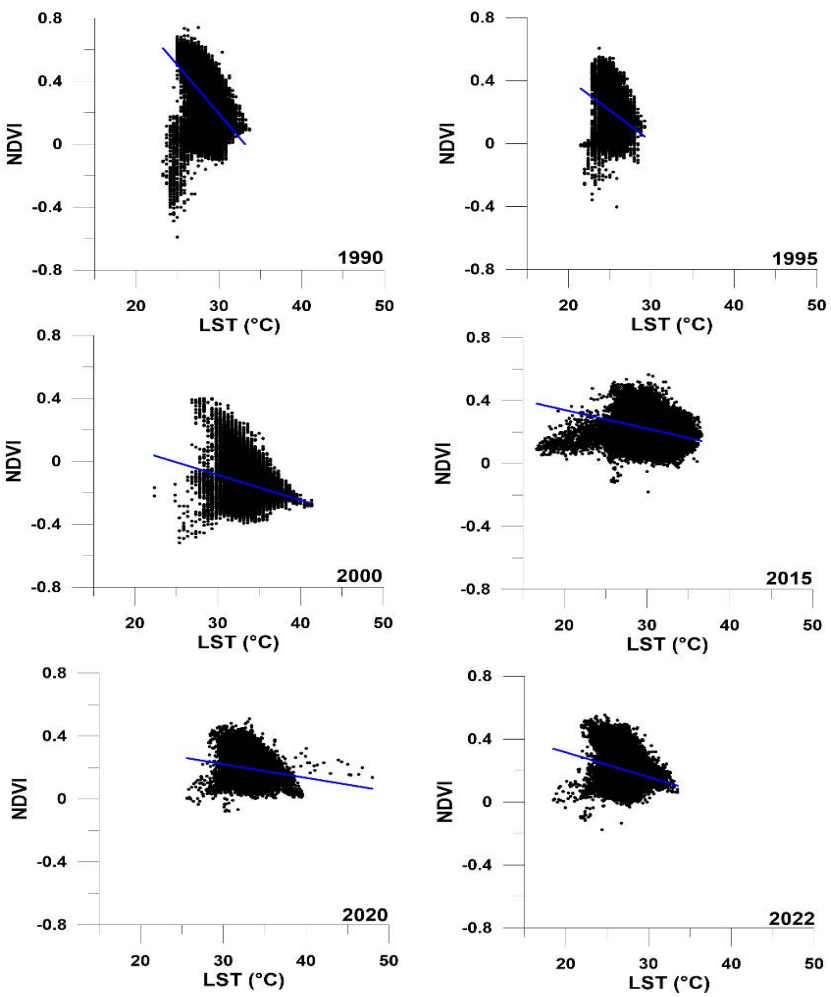

Figure 6. Relationship between NDVI and LST for the case study in the years: a) 1990; b) 1995; c) 2000; d) 2015; e) 2020; f) 2022. Source: Preparation by the authors.

ANÁLISIS ESPACIOTEMPORAL DE ISLAS DE CALOR APLICADO EN LA CIUDAD COSTERA DE SAN FRANCISCO DE CAMPECHE, MÉXICO
ROMÁN CANUL-TURRIZA, KARIANNA AKÉ-TURRIZA, OSCAR MAY-TZUC, MARIO JIMÉNEZ-TORRES
REVISTA URBANO Nº 49 / MAYO 2024 - OCTUBRE 2024
PÁG. 8 - 23
ISSN 0717 - 3997 / 0718 - 3607

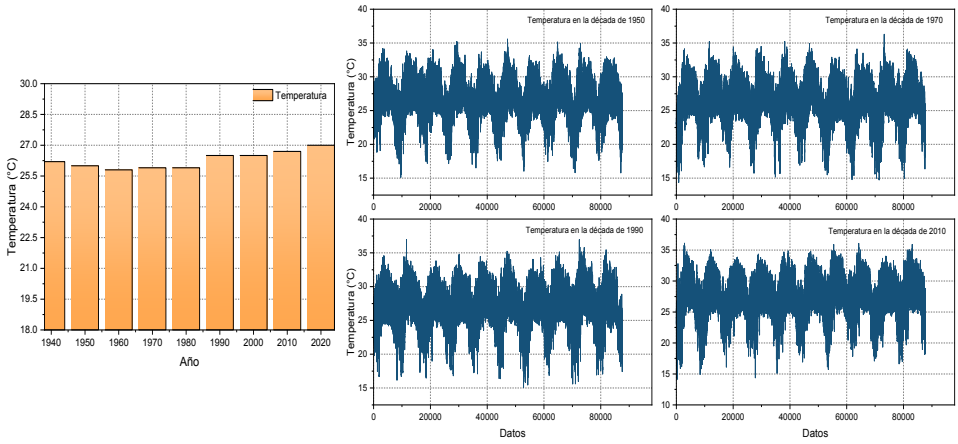

Figure 7. Temperature behavior in SFC in the different decades of study. Source: Preparation by the authors

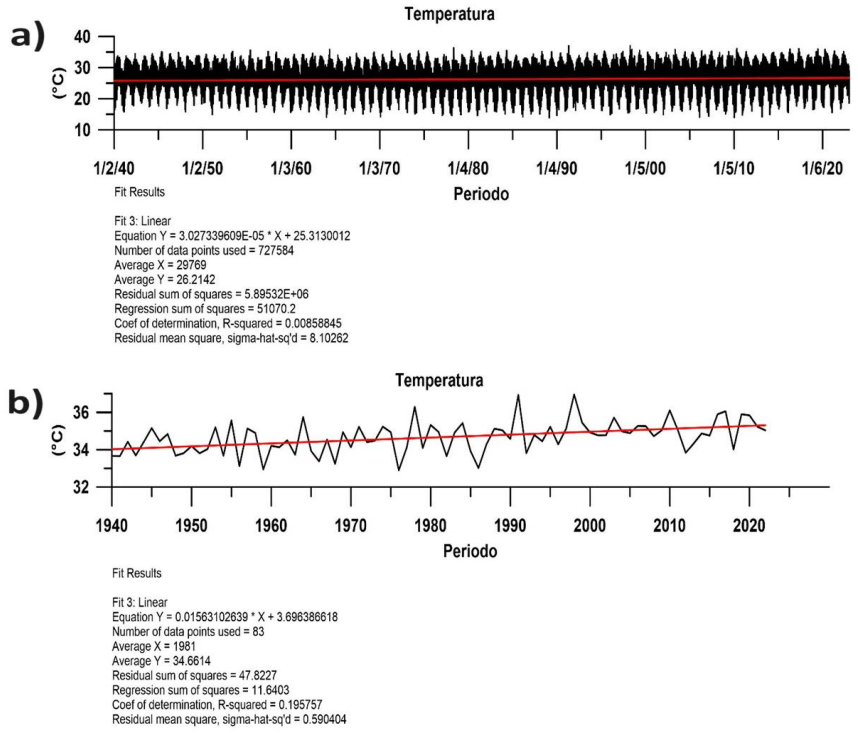

Figure 8. Hourly temperature data series in the period January 1940 - December 2022. b) Series of annual maximum temperature values between 1940 and 2022. Source: Preparation by the authors.

When vegetation affects the distribution of the LST, a reasonable approach to determine the spatiotemporal changes is to identify the relationships between the LST and the NDVI. Figure 6 illustrates the negative relationship between the NDVI and LST values. Between 1990 and 1995, the LST values did not exceed 35°C, while the NDVI was distributed between 0.8 and -0.1 on average. This results in negative and very steep regression slopes, suggesting vegetation softened the thermal effect. The correlations tend to be more horizontal from

ANÁLISIS ESPACIOTEMPORAL DE ISLAS DE CALOR APLICADO EN LA CIUDAD COSTERA DE SAN FRANCISCO DE CAMPECHE, MÉXICO
ROMÁN CANUL-TURRIZA, KARIANNA AKÉ-TURRIZA, OSCAR MAY-TZUC, MARIO JIMÉNEZ-TORRES
REVISTA URBANO Nº 49 / MAYO 2024 - OCTUBRE 2024
PÁG. 8 - 23
ISSN 0717 - 3997 / 0718 - 3607

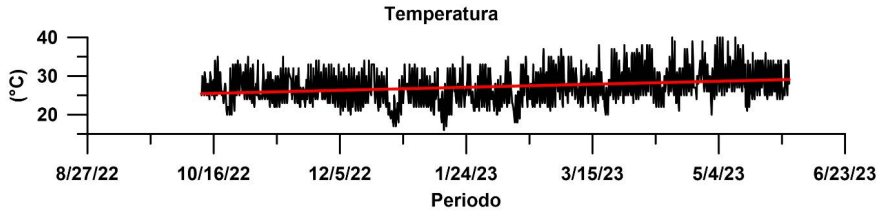

Figure 9. Data record of the climatological season; the date format is month/day/year. Source: Preparation by the authors.

2000 due to an increase in temperature values, which reach 40°C, and a decrease in noticeable vegetation, which acquires an average maximum NDVI between 0.4 and a minimum of up to -0.4. From 2015 to 2020, the NDVI values are grouped in intervals of 0 and 0.4, with some minimum values reaching -0.2 or 0.5. The temperature remains close to 40°C; in 2020, it even approaches 50°C. For 2022, the trend of the NDVI values is maintained, and a reduction in the (surface) temperature values is observed, reaching values close to 35°C. This reduction of the NDVI is indicative of deforestation due to the urban area's expansion and the temperature increases, which indicate the presence of UHIs in the city.

Surface temperature time series

The temperature data were acquired at a location in the coastal zone 15 km away from the city, derived from the resolution of the meshing of the ERAS model, corresponding to 0.25°C, at intervals of 28km. Figure 7 shows the temperature behavior from the annual perspective and the analysis in four specific decades (1950, 1970, 1990, and 2010). There has been a gradual increase in temperature since 1970, an increase in maximum temperatures in recent decades, and a decrease in minimum temperatures due to thermal warming in the region.

Figure 8 above shows the temperature series with an average value of 26.21 °C, a minimum of 14.01 °C, and a maximum of 36.95 °C, reached in 2020. According to the graph below, the maximum recorded value was 33.66°C in 1940, while in 2020, it was 35.83°C. Likewise, the series' trend line indicates that the temperature has increased by 1.30°C and reached highs of 34.66°C.

Figure 9 presents the data for October 2022 to May 31st, 2023, recording a minimum temperature of 16°C, a maximum of 40°C, and an average of 27.3°C. An upward trend is observed that begins in April and extends until the middle of May when the values reach 40 °C

VI. DISCUSSION

The results for the case study exhibit an interrelation between the lack of urban design and planning, which, together with the UHIs, results in high thermal retention of solar radiation impacting buildings, pavements, materials, and surfaces, a situation very similar to that reported by Tian et al. (2021). This also coincides with what was reported by Han et al. (2022), who find that coastal cities experience the most changes because emerging cities experience growth without policies or planning, causing rapid expansions in proportion, density, and regularity. This is contrary to cities with planned development, where more natural areas such as green surfaces and urban parks are built to improve the environment and reduce thermal stress. This supports the hypothesis that the analysis of population growth contributes to identifying the UHIs.

In the case study, the effect of UHIs is increased due to the relative humidity typical of coastal cities, which can vary from 60% to 100% throughout the day. For the case of Singapore, Chew et al. (2021) mention that relative humidity, being related to temperature increases during the day and night, indicates a daily variation of up to 3°C they also use data measured in the field with stations.

The use of images to identify the UHIs is widespread. For example, in the city of Thessaloniki, Greece (Giannaros & Melas, 2012), images were used to identify the UHIs. They also used temperature data measured at stations. However, Giannaros and Melas (2012) incorporated wind speed and thermal comfort into their analysis, finding variations of up to 4 °C.

On the other hand, the Landsat imaging application in the study conducted in Istanbul by Dihkan et al. (2015) stands out since they analyze the 1984 – 2011 period to find the LST, identifying the land uses/cover (LULC) and its temporal and spatial changes, finding a relationship between LST and LULC, which originate the HUS with temperatures close to 50°C. In the city of Muscat, Oman, the authors Charabi and Bakhit (2011) use meteorological observations to infer the spatio–temporal changes analyzed during one year. These studies support the hypothesis that

satellite images can successfully quantify historical surface temperature and vegetation coverage changes.

The phenomenon of UHIs has adverse effects on the social-urban ecosystem, such as an increase in the electricity consumption in buildings, a reduction of thermal comfort, and a decrease in air quality, affecting the health of residents and leading to higher mortality. A recent study in the metropolitan city of Bangkok (Thailand) on physical factors driving the urban heat island found that the average annual temperature of a city with more than one million inhabitants is between 1K and 3K higher than that of the surrounding rural areas (Khamchiangta & Dhakal, 2019).

When the intensification of UHIs occurs, there is an increase in the mortality of children and older adults, as well as in respiratory and cardiovascular diseases and even cancer (Hidalgo García & Arco Díaz, 2021; Hidalgo-García & Arco-Díaz, 2023; Yao et al., 2022). Changes in land use patterns, combined with population growth and the heat generated by human activity, drastically alter the climate as Ullah et al. (2019) have evidenced. This situation is analogous to that observed in SFC, where land use changes, population and urban growth have changed the city's temperature.

The studies examined on UHIs agree that urbanization causes changes in the physical characteristics of the natural landscape and urban land use, resulting in the disappearance of large areas of vegetation and modifying the local climate (Zhao et al., 2011). In the San Francisco de Campeche case study, the NDVI allowed seeing the areas with the most changes, finding a relationship between the LST and vegetation coverage, similar to that of Hidalgo García & Arco Díaz (2021) and Hu et al. (2020), who associated NDVI with LST, finding a negative correlation; i.e., there is a reduction in NDVI values as LST values increase. This confirms the hypothesis that changes in vegetation cover will facilitate the identification of UHI areas.

In SFC, it is seen that the reduction in NDVI values is due to the construction of housing units. This can be compared with what is documented by Ciacci et al. (2022) that, in cities, the changes generated by the construction sector represent 27% of global greenhouse gas emissions. Therefore, diverse mitigation strategies have been proposed and applied to reduce the risk of UHIs. The ones that stand out are urban green spaces, green roofs, vertical greening or green walls, water bodies, cold materials, and changes in urban geometry (Ciacci et al., 2022). Planning and design that modify the characteristics of the surrounding environment could reduce the UHIs. Replacing trees and vegetation with less permeable material surfaces minimizes the natural effects of shading, water evaporation from the soil, and leaf evapotranspiration, so the reverse process would maximize them.

Studies have been conducted to maximize the natural effects of shading strategies, focusing on UHI mitigation measures and their impact on building energy consumption and outdoor thermal comfort (Tian et al., 2021). The implementation of sustainable urban infrastructure, sustainable rain management, and reduction of anthropogenic heat have been proposed, as well as the implementation of mitigation measures in construction, such as protection from solar radiation, minimization of heat infiltration, maintenance of thermal comfort, and the planning of urban areas together with urban development measures such as reforestation, green infrastructure, and reduction of anthropogenic heat (Leal Filho et al., 2017). In addition, it can influence public policies, certifications, and regulations, which allow, as well as the methodology applied in Europe on optimal profitability (European Parliament, 2010), outlining the most cost-effective measures to rebuild buildings, focusing on economic aspects or interventions to achieve an NZEB (Nearly zero–energy buildings) standard, or energy and environmental certifications in the urban environment. An example of them is the Italian regulations, which regulate the development of the urban environment to comply with the Kyoto Protocols, highlighting the role of trees (Ciacci et al., 2022). However, this lacks strategies, methodologies, regulations, and public policies that reduce the effects of UHIs.

In the last three decades, San Francisco de Campeche has experienced an increase in its temperature, which has resulted in a 40% increase in electricity consumption, as reported by SENER (2023), coinciding with what was pointed out by Tian et al. (2021) who indicate that, in countries with warm climates, every 1°C increase leads to a 1.66% increase in electricity consumption. Implementing any of the strategies above in the case study could substantially impact the thermal-urban environment if used primarily in the project's design stage.

Although no strategy for UHI reduction is applied in this research, some implemented in other regions that, due to SFC's characteristics, could be practical and replicable are proposed. An example of this is that urban greening can purify the air, regulate the temperature, and improve the urban ecosystem. On the other hand, urban green space lowers the air temperature, mitigates pollution, and reduces the energy used for cooling. The use of green roofs can influence the urban environment since they represent between 20% and 25% of a city's surface (Besir & Cuce, 2018). They can also reduce indoor temperatures on the top floor by up to 3.4°C (Tam et al., 2016).

In Hong Kong, a study on urban heat island mitigation strategies showed that with 60% green cover, the air

ANÁLISIS ESPACIOTEMPORAL DE ISLAS DE CALOR APLICADO EN LA CIUDAD COSTERA DE SAN FRANCISCO DE CAMPECHE, MÉXICO
ROMÁN CANUL-TURRIZA, KARIANNA AKÉ-TURRIZA, OSCAR MAY-TZUC, MARIO JIMÉNEZ-TORRES
REVISTA URBANO Nº 49 / MAYO 2024 - OCTUBRE 2024
PÁG. 8 - 23
ISSN 0717 - 3997 / 0718 - 3607

ANÁLISIS ESPACIOTEMPORAL DE ISLAS DE CALOR APLICADO EN LA CIUDAD COSTERA DE SAN FRANCISCO DE CAMPECHE, MÉXICO
ROMÁN CANUL-TURRIZA, KARIANNA AKÉ-TURRIZA, OSCAR MAY-TZUC, MARIO JIMÉNEZ-TORRES
REVISTA URBANO Nº 49 / MAYO 2024 - OCTUBRE 2024
PÁG. 8 - 23
ISSN 0717 - 3997 / 0718 - 3607

Figure 10. Intervention proposals. a) Before, b) Reforestation, c) Before, d) Green wall placement. Source: Preparation by the authors.

temperature could be reduced between 0.65°C-1.45°C and the annual energy savings were estimated at $3.4x10^7$kWh and $7.6x10^7$kWh, respectively (Peng & Jim, 2015). In the same way, green walls are smaller in size, have high aesthetic value, and can mitigate UHIs by reducing the wall's temperature to save energy, with thermal insulation provided by vegetation, cooling evapotranspiration, and screening against the wind. Pan and Chu (2016) showed that a green wall can save 16% of a building's energy consumption.

Figure 10 shows a before-and-after of a proposal to reforest an urban sector and the proposal to place a green wall in a house. The sector is on 59th Street, located in the historic center. This street connects the Puerta de Mar with the Puerta de Tierra of the walled city, becoming the city's most popular and crowded meeting point, the so-called "heart of the Historic Center of Campeche." The Figure's house represents the modern constructions in San Francisco de Campeche.

Finally, urban planning can improve the urban climate by meeting the needs of residents (Zhao et al., 2011). Together with urban design, this has a realistic environmental meaning and can mitigate the effect of UHIs in some urban regions by optimizing urban morphology (Q. Hu et al., 2016). The size, geometric shape, and vegetation cover are the urban morphology factors that impact the thermal stress of the city (Liang et al., 2021)Given this, SFC requires urban planning that allows it to develop and decrease UHIs. The results of this study provide a watershed that will enable deepening the analysis of UHIs, from their origin to reduction strategies. This will be useful for urban planners (engineers, architects, among others), public health officials, and government actors.

VII. CONCLUSIONS

The UHI analysis has been consolidated as an indispensable component in understanding the current urban climate. This research reveals the importance of complementing traditional climate and weather studies, such as the agricultural calendar and rainfall periods, among others, with historical temperature analyses and satellite images. These provide a crucial perspective on addressing the challenges of unplanned urban growth. Integrating data on UHIs with urban planning and design observations is presented as a comprehensive approach to mitigating the adverse effects of disorganized urban development.

The UHIs identified in the city of SFC focus on areas with a high density of urban infrastructure, where the presence of buildings is predominant and vegetation is scarce. This urban concentration has been associated with a significant increase in surface temperature, with a rise of 6°C recorded from 1990 to 2022. At the same time, a marked decrease in vegetation cover has been observed, quadrupling the values of the Normalized Difference Vegetation Index in the 0 – 0.25 class in the same period. These findings reflect an increasing trend in temperature, especially evidenced by the series of annual maximum values of the period.

The UHI in SFC is due to environmental degradation that currently disturbs the population's comfort, mainly in April. This increase in temperature causes an increase in electricity consumption to maintain thermal comfort, in addition to generating adverse effects on public health.

Additional variables that may influence the formation and intensity of UHIs are suggested. Relative humidity and wind speed are important factors that can modulate the effects of UHIs and should be considered in future studies. In addition, a detailed thermal comfort analysis provides a more complete understanding of how climatic conditions affect the subjective perception of temperature and human well-being. Identifying the periods of greatest discomfort and comparing these parameters during the day and night generates a more accurate assessment of the risks associated with UHIs and guides adaptation and mitigation strategies.

Ultimately, to effectively address the challenges caused by UHIs and to improve the quality of urban habitat, it is necessary to implement various political strategies, leading to the modification of public policies based on urban planning results, which considers short-term actions such as revegetation with local vegetation and the creation of green spaces, in addition to the incorporation of innovative interventions such as the development of green infrastructures and walls. By promoting urban vegetation and improving vegetation cover, air temperatures can be reduced, UHI's effects can be mitigated, and profitable and sustainable environments for urban dwellers can be generated. These interventions reduce energy consumption, improve urban biodiversity, and create recreational and functional public spaces.

In this way, UHI analysis emerges as a crucial research area to address the different challenges of disorganized urban growth. By integrating data on UHI with urban planning and design considerations, progress is demonstrated toward sustainable, resilient, and livable cities capable of mitigating the adverse impacts of urban development without control for present and future generations.

VIII. REFERENCES

Besir, A. B., & Cuce, E. (2018). Green roofs and facades: A comprehensive review. *Renewable and Sustainable Energy Reviews*, *82*, 915–939. https://doi.org/10.1016/j.rser.2017.09.106

Charabi, Y., & Bakhit, A. (2011). Assessment of the canopy urban heat island of a coastal arid tropical city: The case of Muscat, Oman. *Atmospheric Research*, *101*(1), 215–227. https://doi.org/https://doi.org/10.1016/j.atmosres.2011.02.010

Chew, L. W., Liu, X., Li, X.-X., & Norford, L. K. (2021). Interaction between heat wave and urban heat island: A case study in a tropical coastal city, Singapore. *Atmospheric Research*, *247*, 105134. https://doi.org/https://doi.org/10.1016/j.atmosres.2020.105134

Ciacci, C., Banti, N., Di Naso, V., Montechiaro, R., & Bazzocchi, F. (2022). Experimentation of Mitigation Strategies to Contrast the Urban Heat Island Effect: A Case Study of an Industrial District in Italy to Implement Environmental Codes. *Atmosphere*, *13*(11), 1808. https://doi.org/10.3390/atmos13111808

Degirmenci, K., Desouza, K. C., Fieuw, W., Watson, R. T., & Yigitcanlar, T. (2021). Understanding policy and technology responses in mitigating urban heat islands: A literature review and directions for future research. *Sustainable Cities and Society*, *70*, 102873. https://doi.org/10.1016/j.scs.2021.102873

Dihkan, M., Karsli, F., Guneroglu, A., & Guneroglu, N. (2015). Evaluation of surface urban heat island (SUHI) effect on coastal zone: The case of Istanbul Megacity. *Ocean & Coastal Management*, *118*, 309–316. https://doi.org/ 10.1016/j.ocecoaman.2015.03.008

Firozjaei, M. K., Sedighi, A., Mijani, N., Kazemi, Y., & Amiraslani, F. (2023). Seasonal and daily effects of the sea on the surface urban heat island intensity: A case study of cities in the Caspian Sea Plain. *Urban Climate*, *51*, 101603. https://doi.org/https://doi.org/10.1016/j.uclim.2023.101603

Giannaros, T. M., & Melas, D. (2012). Study of the urban heat island in a coastal Mediterranean City: The case study of Thessaloniki, Greece. *Atmospheric Research*, *118*, 103–120. https://doi.org/https://doi.org/10.1016/j.atmosres.2012.06.006

Han, W., Tao, Z., Li, Z., Cheng, M., Fan, H., Cribb, M., & Wang, Q. (2022). Effect of Urban Built-Up Area Expansion on the Urban Heat Islands in Different Seasons in 34 Metropolitan Regions across China. *Remote Sensing*, *15*(1), 248. https://doi.org/10.3390/rs15010248

Hidalgo García, D., & Arco Díaz, J. (2021a). Modeling of the Urban Heat Island on local climatic zones of a city using Sentinel 3 images: Urban determining factors. *Urban Climate*, *37*. https://doi.org/https://doi.org/10.1016/j.uclim.2021.100840

Hidalgo-García, D., & Arco-Díaz, J. (2023). Spatiotemporal analysis of the surface urban heat island (SUHI), air pollution and disease pattern: an applied study on the city of Granada (Spain). *Environmental Science and Pollution Research*, *30*(20), 57617–57637. https://doi.org/10.1007/s11356-023-26564-7

Hu, Q., Zhang, R., & Zhou, Y. (2016). Transfer learning for short-term wind speed prediction with deep neural networks. *Renewable Energy*, *85*, 83–95. https://doi.org/10.1016/j.renene.2015.06.034

REVISTA URBANO Nº 49 / MAYO 2024 - OCTUBRE 2024
PÁG. 8 - 23
ISSN 0717 - 3997 / 0718 - 3607

ANÁLISIS ESPACIOTEMPORAL DE ISLAS DE CALOR APLICADO EN LA CIUDAD COSTERA DE SAN FRANCISCO DE CAMPECHE, MÉXICO
ROMÁN CANUL-TURRIZA, KARIANNA AKÉ-TURRIZA, OSCAR MAY-TZUC, MARIO JIMÉNEZ-TORRES
REVISTA URBANO Nº 49 / MAYO 2024 - OCTUBRE 2024
PÁG. 8 - 23
ISSN 0717 - 3997 / 0718 - 3607

Hu, Y., Dai, Z., & Guldmann, J.-M. (2020). Modeling the impact of 2D/3D urban indicators on the urban heat island over different seasons: A boosted regression tree approach. *Journal of Environmental Management*, *266*, 110424. https://doi.org/10.1016/j.jenvman.2020.110424

INEGI. (2020). Panorama sociodemográfico de México 2020: Campeche.

INEGI. (2022). Aspectos Geográficos: Campeche 2021.
Kassomenos, P., Kissas, G., Petrou, I., Begou, P., Khan, H. S., & Santamouris, M. (2022). The influence of daily weather types on the development and intensity of the urban heat island in two Mediterranean coastal metropolises. *Science of The Total Environment*, *819*, https://doi.org/https://doi.org/10.1016/j.scitotenv.2022.153071

Khamchiangta, D., & Dhakal, S. (2019). Physical and non-physical factors driving urban heat island: Case of Bangkok Metropolitan Administration, Thailand. *Journal of Environmental Management*, *248*. https://doi.org/10.1016/j.jenvman.2019.109285

Khare, V. R., Vajpai, A., & Gupta, D. (2021). A big picture of urban heat island mitigation strategies and recommendation for India. *Urban Climate*, *37*. https://doi.org/https://doi.org/10.1016/j.uclim.2021.100845

Kim, S. W., & Brown, R. D. (2021). Urban heat island (UHI) intensity and magnitude estimations: A systematic literature review. *Science of The Total Environment*, *779*. https://doi.org/10.1016/j.scitotenv.2021.146389

Leal Filho, W., Echevarria Icaza, L., Emanche, V., & Quasem Al-Amin, A. (2017). An Evidence-Based Review of Impacts, Strategies and Tools to Mitigate Urban Heat Islands. *International Journal of Environmental Research and Public Health*, *14*(12), 1600. https://doi.org/10.3390/ijerph14121600

Li, H., Meier, F., Lee, X., Chakraborty, T., Liu, J., Schaap, M., & Sodoudi, S. (2018). Interaction between urban heat island and urban pollution island during summer in Berlin. *Science of The Total Environment*, *636*, 818–828. https://doi.org/10.1016/j.scitotenv.2018.04.254

Li, X., Li, W., Middel, A., Harlan, S. L., Brazel, A. J., & Turner, B. L. (2016). Remote sensing of the surface urban heat island and land architecture in Phoenix, Arizona: Combined effects of land composition and configuration and cadastral–demographic–economic factors. *Remote Sensing of Environment*, *174*, 233–243. https://doi.org/10.1016/j.rse.2015.12.022

Liang, Z., Huang, J., Wang, Y., Wei, F., Wu, S., Jiang, H., Zhang, X., & Li, S. (2021). The mediating effect of air pollution in the impacts of urban form on nighttime urban heat island intensity. *Sustainable Cities and Society*, *74*. https://doi.org/10.1016/j.scs.2021.102985

Luo, Y., & He, J. (2021). Evaluating the heat island effect in a planned residential area using planning indicators. *Journal of Building Engineering*, *43*, https://doi.org/10.1016/j.jobe.2021.102473

Ma, Y., Lauwaet, D., Kouti, A., & Verbeke, S. (2023). A toolchain to evaluate the impact of urban heat island and climate change on summer overheating at district level. *Urban Climate*, *51*, 2. https://doi.org/10.1016/j.uclim.2023.101602

Ortiz Porangaba, G. F., Teixeira, D. C. F., Amorim, M. C. de C. T., Silva, M. H. S. & Dubreuil, V. (2021). Modeling the urban heat island at a winter event in Três Lagoas, Brazil. *Urban Climate*, *37*. https://doi.org/10.1016/j.uclim.2021.100853

Pan, L., & Chu, L. M. (2016). Energy saving potential and life cycle environmental impacts of a vertical greenery system in Hong Kong: A case study. *Building and Environment*, *96*, 293–300. https://doi.org/https://doi.org/10.1016/j.buildenv.2015.06.033

Parlamento Europeo (2010). European Parliament and Council of the European Union - Directive 2010/31/EU. Unión Europea.

Peng, L. L. H., & Jim, C. Y. (2015). Economic evaluation of green-roof environmental benefits in the context of climate change: The case of Hong Kong. *Urban Forestry & Urban Greening*, *14*(3), 554–561. https://doi.org/https://doi.org/10.1016/j.ufug.2015.05.006

Qiu, J., Li, X., & Qian, W. (2023). Optimizing the spatial pattern of the cold island to mitigate the urban heat island effect. *Ecological Indicators*, *154*. https://doi.org/10.1016/j.ecolind.2023.110550

SEDATU (2020). *Programa municipal para el desarrollo urbano: Campeche 2020-2040*. Secretaría de Desarrollo Agrario, Rural y Urbano.

SENER (2023). *Sistema de Información Energética*. Secretaría de Energía. https://sie.energia.gob.mx/bdiController.do?action=cuadro&subAction=applyOptions

Singh, N., Singh, S., & Mall, R. K. (2020). Urban ecology and human health: implications of urban heat island, air pollution and climate change nexus. In *Urban Ecology* (pp. 317–334). Elsevier Inc. https://doi.org/10.1016/b978-0-12-820730-7.00017-3

Tam, V. W. Y., Wang, J., & Le, K. N. (2016). Thermal insulation and cost effectiveness of green-roof systems: An empirical study in Hong Kong. *Building and Environment*, *110*, 46–54. https://doi.org/https://doi.org/10.1016/j.buildenv.2016.09.032

Tan, J. K. N., Belcher, R. N., Tan, H. T. W., Menz, S., & Schroepfer, T. (2021). The urban heat island mitigation potential of vegetation depends on local surface type and shade. *Urban Forestry & Urban Greening*, *62*, 127128. https://doi.org/https://doi.org/10.1016/j.ufug.2021.127128

Tian, L., Li, Y., Lu, J., & Wang, J. (2021). Review on Urban Heat Island in China: Methods, Its Impact on Buildings Energy Demand and Mitigation Strategies. *Sustainability*, *13*(2), 762. https://doi.org/10.3390/su13020762

Ullah, S., You, Q., Ullah, W., Hagan, D. F. T., Ali, A., Ali, G., Zhang, Y., Jan, M. A., Bhatti, A. S., & Xie, W. (2019). Daytime and nighttime heat wave characteristics based on multiple indices over the China–Pakistan economic corridor. *Climate Dynamics*, *53*(9), 6329–6349. https://doi.org/10.1007/s00382-019-04934-7

United States Geological Survey. (n.d.). http://earthexplorer.usgs.gov/

Vasenev, V., Varentsov, M., Konstantinov, P., Romzaykina, O., Kanareykina, I., Dvornikov, Y., y Manukyan, V. (2021). Projecting urban heat island effect on the spatial-temporal variation of microbial respiration in urban soils of Moscow megalopolis. *Science of The Total Environment*, 786. https://doi.org/https://doi.org/10.1016/j.scitotenv.2021.147457

Wang, R., Hou, H., Murayama, Y., & Derdouri, A. (2020). Spatiotemporal Analysis of Land Use/Cover Patterns and Their Relationship with Land Surface Temperature in Nanjing, China. *Remote Sensing*, *12*(3), 440. https://doi.org/10.3390/rs12030440

Xu, L., Wang, J., Xiao, F., El-Badawy, S., & Awed, A. (2021a). Potential strategies to mitigate the heat island impacts of highway pavement on megacities with considerations of energy uses. *Applied Energy*, *281*. https://doi.org/10.1016/j.apenergy.2020.116077

Xu, X., Pei, H., Wang, C., Xu, Q., Xie, H., Jin, Y., Feng, Y., Tong, X., & Xiao, C. (2023). Long-term analysis of the urban heat island effect using multisource Landsat images considering inter-class differences in land surface temperature products. *Science of The Total Environment*, *858*. https://doi.org/https://doi.org/10.1016/j.scitotenv.2022.159777

Yao, L., Sun, S., Song, C., Wang, Y., & Xu, Y. (2022). Recognizing surface urban heat 'island' effect and its urbanization association in terms of intensity, footprint, and capacity: A case study with multi-dimensional analysis in Northern China. *Journal of Cleaner Production*, *372*. https://doi.org/https://doi.org/10.1016/j.jclepro.2022.133720

Yun, G. Y., Ngarambe, J., Duhirwe, P. N., Ulpiani, G., Paolini, R., Haddad, S., Vasilakopoulou, K., & Santamouris, M. (2020). Predicting the magnitude and the characteristics of the urban heat island in coastal cities in the proximity of desert landforms. The case of Sydney. *Science of The Total Environment*, *709*. https://doi.org/10.1016/j.scitotenv.2019.136068

Zhao, C., Fu, G., Liu, X., & Fu, F. (2011). Urban planning indicators, morphology and climate indicators: A case study for a north-south transect of Beijing, China. *Building and Environment*, *46*(5), 1174–1183. https://doi.org/https://doi.org/10.1016/j.buildenv.2010.12.00

ANÁLISIS ESPACIOTEMPORAL DE ISLAS DE CALOR APLICADO EN LA CIUDAD COSTERA DE SAN FRANCISCO DE CAMPECHE, MÉXICO
ROMÁN CANUL-TURRIZA, KARIANNA AKÉ-TURRIZA, OSCAR MAY-TZUC, MARIO JIMÉNEZ-TORRES
REVISTA URBANO Nº 49 / MAYO 2024 - OCTUBRE 2024
PÁG. 8 - 23
ISSN 0717 - 3997 / 0718 - 3607